



The design and microfabrication of a sub 100 mg insect-scale flapping-wing robot

Yang Zou, Weiping Zhang , Xijun Ke, Xingliang Lou, Sui Zhou

National Key Laboratory of Science and Technology on Micro/Nano Fabrication, Key Laboratory for Thin Film and Micro Fabrication of the Ministry of Education, Shanghai Key Laboratory of Navigation and Location-Based Services, Department of Micro-Nano Electronics, School of Electronic Information and Electrical Engineering, Shanghai Jiao Tong University, Shanghai 200240, People's Republic of China

 E-mail: zwp37@163.com

Published in Micro & Nano Letters; Received on 16th November 2016; Revised on 7th January 2017; Accepted on 18th January 2017

A piezo-actuated self-lifting insect inspired flapping-wing robot is presented. A novel method is presented in the work, which has taken into account the difficulties and the precision of assembly among micro components. Each component is properly designed and reasonably arranged to reduce the assembly difficulties of such insect-scale robot. Specifically, the design of the piezoelectric actuator has taken into account the electrical isolation and assembly issues. The transmission and the airframe are integrated into one component to avoid assembly difficulties. Fibre directions of wing veins are reasonably arranged to possess high strength and stiffness. As a result, this robot, which weighs 84 mg with a wingspan of 35 mm, can generate sufficient thrust to take off with a flapping amplitude approximately $\pm 60^\circ$ under the resonant wingbeat frequency of 100 Hz.

1. Introduction: Over the past few decades, many researchers have been working on the exploration of insect flight mechanisms [1, 2] and the development of insect inspired micro aerial vehicles (MAVs) [3–11]. Fortunately, researches on biomimetic flying robots have made unprecedented progress in the past few years. For example, the Harvard Microrobotics Lab has realised the first takeoff of a piezo-actuated robotic insect [4]. AeroVironment's Nano Hummingbird has successfully demonstrated hovering and forward flight through an external controller [5]. The Purdue Bio-Robotics Lab has developed a flapping-wing MAV driven by a pair of high-frequency electromagnetic actuators [6, 7]. Shanghai Jiao Tong University has successfully created a self-lifting, sub 100 mg, flapping-wing robot driven by an electromagnetic actuator [8].

There are some issues that arise with scaling down mechanical structures and systems. For insect-scale MAVs (generally wingspan < 5 cm, weight < 1 g), components such as actuators and revolute joints for large-scale systems become challenging since the surface forces begin to play a more important role than body functions. The structural design, microfabrication and assembly for insect-scale flapping-wing robots are still quite difficult at present.

In this Letter, on the basis of laser processing, a new approach is developed to create insect-scale flapping-wing robots. By using this method, a self-lifting sub 100 mg flapping-wing robot is created.

2. Design and fabrication

2.1. Overall design: The insect-scale flapping-wing robot consists of a piezoelectric actuator, a transmission together with the airframe, a pair of wings and some auxiliary components, as shown in Fig. 1. Each wing is glued to each side of the transmission, respectively. The flexible hinge at the wing root allows its passive rotation which results from the inertia forces and the aerodynamic forces and results in lift producing.

2.2. Piezoelectric actuator: The shape of the piezoelectric actuator is according to the design of Wood [4]. For the piezoelectric actuator in this Letter, the structure is specially modified. Firstly, the head of it is deliberately designed to insert into the square hole of the transmission. Secondly, its tail is designed with two small holes for assembly with the airframe. Thirdly, glass fibre is used in both ends of the actuator to electrically isolate itself from the other components of the robot. Only a small part of carbon fibre is revealed to serve as the electrode.

The piezoelectric actuator is fabricated from seven flat sheets by a process of laser microfabrication. As shown in Fig. 2, firstly, all of the flat sheets [127 μm thick PbZrTiO₃ (PZT)-5H from the Piezo Systems, 120 μm thick S15000 glass fibre material and 40 μm thick USN04000 carbon fibre material from the Weihai Guangwei] are patterned by UV laser to obtain desired plane shapes. Then, according to the pre-designed location holes and grooves, the flat sheets are laminated together in a particular order. Under the condition of high temperature and high pressure, epoxy resin in the carbon fibre and the glass fibre cures and bonds the seven sheets together. Finally, the piezoelectric actuator is cut and released by UV laser.

2.3. Transmission and airframe: The role of the transmission is to transform actuator reciprocating vibrations into wing flapping motions. Inspired by the flapping mechanism of real insects as shown in Fig. 3a [8], four-bar systems with flexible hinges are designed to serve as the transmission of the robot (Fig. 3b). However, the feature sizes and the global sizes of the transmission are relatively small, which will result in many

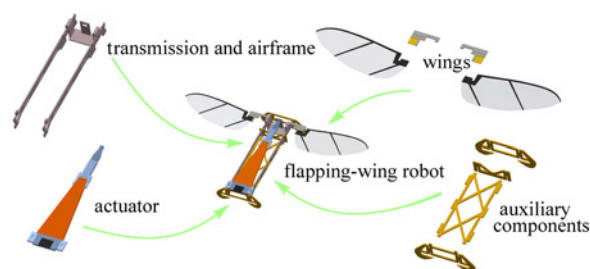


Fig. 1 CAD model of the whole robot and all its components

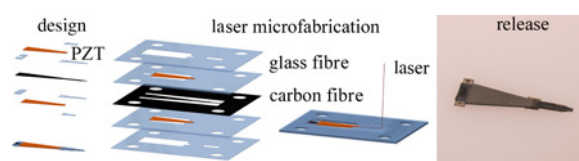


Fig. 2 Design, fabrication and release of the piezoelectric actuator

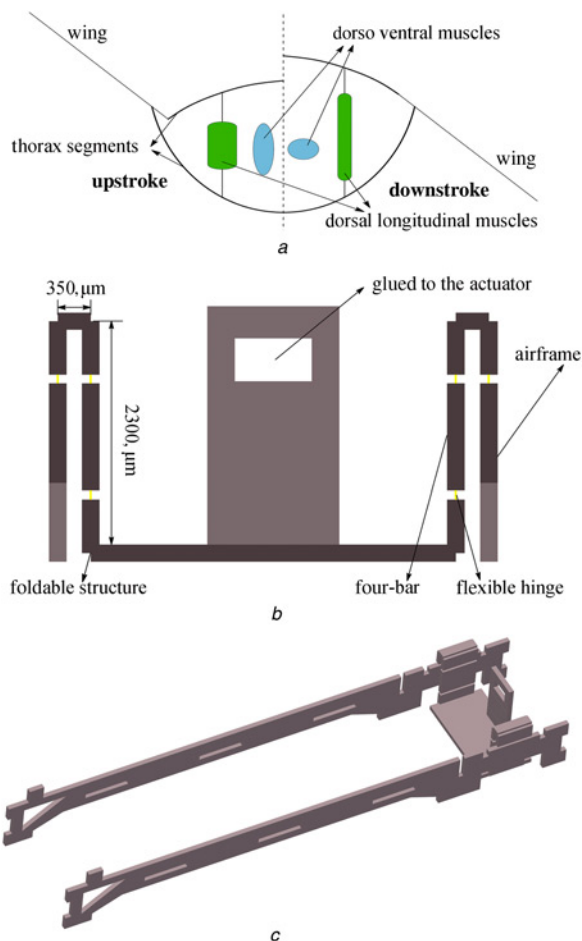


Fig. 3 Design of the transmission and airframe

a Schematic diagram of the insect thorax [8]

b Cutaway view of the transmission

c CAD model of the transmission together with the airframe

assembly problems between the transmission and the airframe. For example, it is very difficult to assemble the transmission with the airframe by a manual process. In addition, the assembly errors have a great influence on the accuracy of the transmission's feature sizes. In this Letter, the transmission and the airframe are integrated into one component to avoid the assembly between these two parts and ensure the accuracy of the transmission's feature sizes, as shown in Fig. 3c.

As shown in Fig. 3b, the fabrication of the transmission consists of two parts: flexible hinges and foldable structures. The flexible hinges can act as 'shafts' while the foldable structures can be

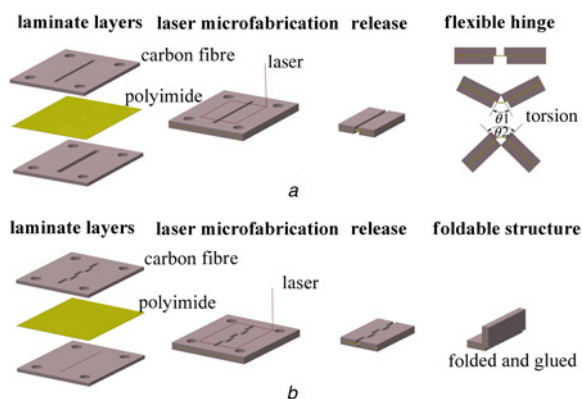


Fig. 4 Microfabrication processes of

a Flexible hinge,

b Foldable structure



Fig. 5 Photos of the transmission together with the airframe before and after folding

used to build three-dimensional shapes. Both of them are made from two layers of 80 μm thick high modulus carbon fibre with a layer of 7.5 μm thick polyimide film sandwiching between them. The carbon fibre layers are regarded as the rigid structural layers and the polyimide film is served as the flexible deformable layer. The fabrication processes of the flexible hinge and the foldable structure are shown in Fig. 4. It is worth emphasised that, once the foldable structures are released, they need to be folded in accordance with the pre-designed creases, and locked by cyanoacrylate adhesive.

For the transmission together with the airframe, it is easy to obtain its laminate plate by using the processes in Fig. 4. Once folded and locked, we can obtain its three-dimensional structure, as shown in Fig. 5.

2.4. Wings: The artificial wing is designed to imitate the wing of drone-fly *Eristalis tenax* as shown in Fig. 6a with reference to the wing in Zou [8]. The carbon fibre (USN05400, 60 μm thick) is chosen to build the wing veins due to its intrinsic high modulus and light weight.

The carbon fibre is unidirectional that the modulus along the fibre direction is much higher than that perpendicular to it. As shown in Fig. 6a, there is a wide angle between the leading edge and the veins. It is impossible to guarantee both of them are along the fibre directions if they are patterned together from a single carbon fibre sheet. It is also difficult to ensure the repeatability and consistency of the wings if the leading edge and the veins are fabricated, respectively, and assembled manually. In this Letter, the leading edge and the veins are patterned in different carbon fibre sheets to guarantee both of them are along the fibre directions, as shown in Fig. 6b. Then, according to the pre-designed location holes, the carbon fibre sheets are laminated together with a layer of 1.5 μm thick polyester sandwiching between them. Finally, the wing is released by UV laser as shown in Figs. 6b and c.

The wing root is made from 60 μm thick carbon fibre and 7.5 μm thick polyimide film with similar processes of the transmission.

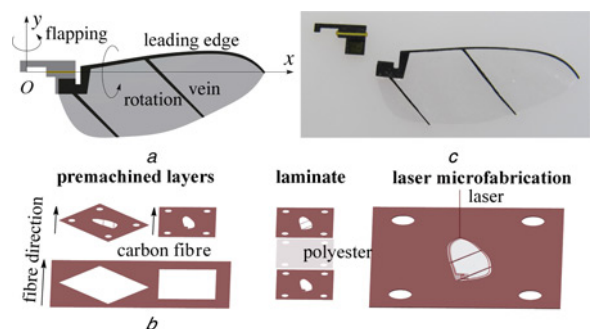


Fig. 6 The artificial wing

a Design of the wing

b Microfabrication processes of the artificial wing

c Photos of the artificial wing and the wing root

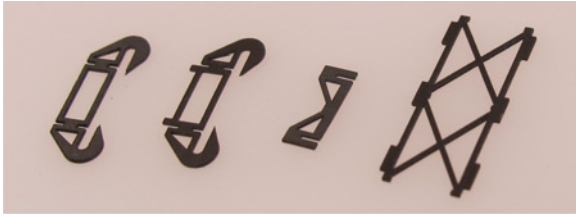


Fig. 7 Photo of the hooks and ribs fabricated by UV laser

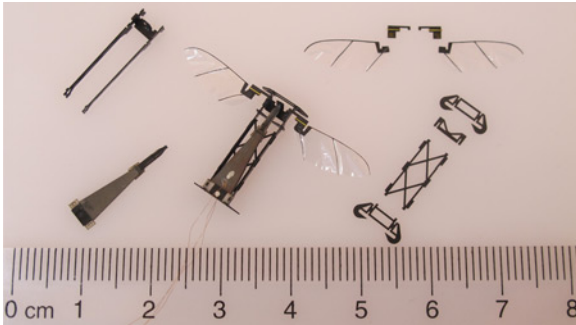


Fig. 8 Photo of all the components and a whole flapping-wing robot

Table 1 Mass of the components

Component	Mass, mg
piezoelectric actuator	55
transmission and airframe	12
double wings	1
wing roots	1
ribs and hooks	9
wiring, epoxy	6
total body	84

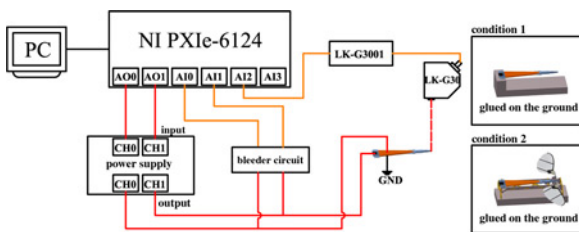


Fig. 9 System diagram of the test for the piezoelectric actuator

2.5. Auxiliary components: The auxiliary components include hooks and ribs. They are made from two layers of 80 μm thick high modulus carbon fibre material with fibre directions orthogonal. As shown in Fig. 7, the ribs and hooks can easily be obtained by using UV laser.

2.6. Results: Each component is manually assembled in a certain order to build the final flapping-wing robot as shown in Fig. 8. Table 1 lists all the components and their corresponding weight.

3. Experiments

3.1. Tests of the piezoelectric actuator: In Fig. 9, the actuator is tested in two different conditions. In Condition 1, the tail of the actuator is fixed on the ground while the head is free with no load. In Condition 2, the actuator is assembled to a whole robot which is glued on the ground. The actuator is excited by a

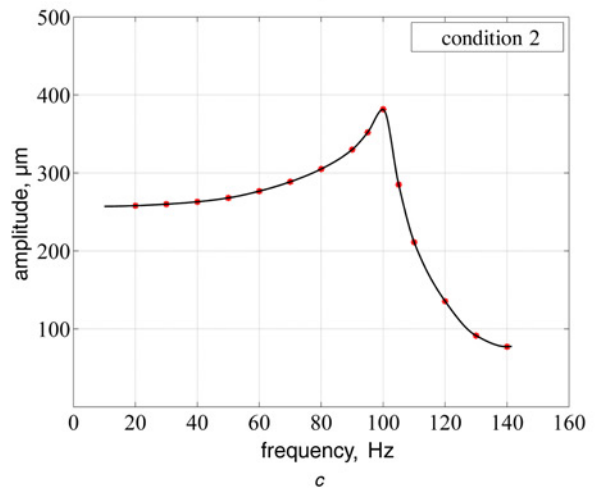
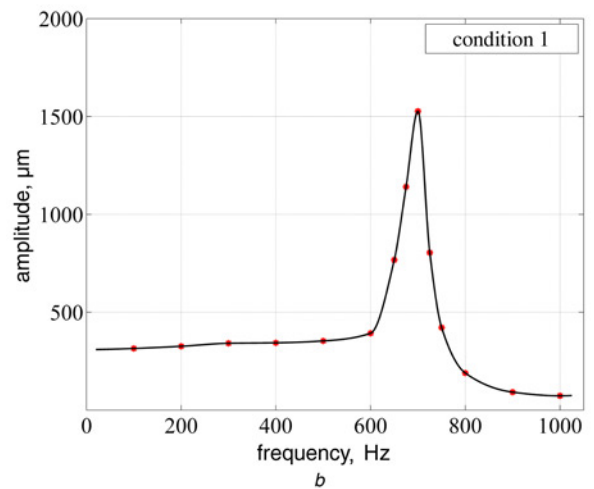
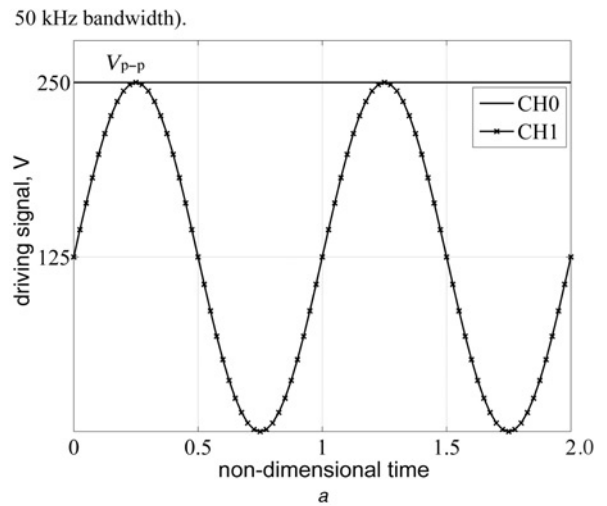


Fig. 10 Performance of the piezoelectric actuator
a Driving signals for the piezoelectric actuator. Displacement amplitude results of the actuator at different driving frequencies
b Condition 1
c Condition 2

two-channel signal generator (NI PXIe-6124) combined with a piezoelectric ceramic transformer. Its tip displacement is measured by a laser displacement sensor (model LK-G30 from KEYENCE, 10 mm sensing range, 0.05 μm reproducibility and 50 kHz bandwidth).

To determine the resonant frequency of the actuator, the peak-to-peak value (V_{p-p} in Fig. 10a) of the driving signal is set

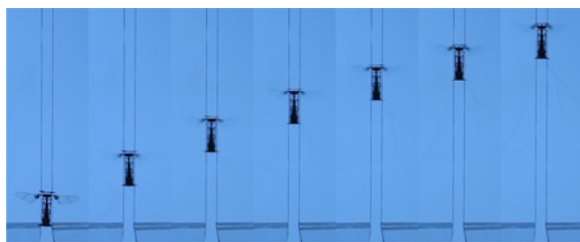


Fig. 11 *Liftoff of the flapping-wing robot. The interval between the images is ~ 1 s*

to 250 V under sweep-frequency mode. As shown in Figs. 10b and c, the resonant frequency of the actuator is ~ 700 Hz with a vibration amplitude of ± 1.5 mm in Condition 1 and it is ~ 100 Hz with a vibration amplitude of ± 380 μ m in Condition 2. In Condition 2, the wings of the robot flap rapidly under the resonant frequency with a flapping amplitude of approximately $\pm 60^\circ$.

3.2. Liftoff of the robot: To isolate the influence of the other degrees of freedom, the robot is constrained by a pair of vertical guide rails. Excited by an external power source (frequency of 100 Hz and V_{P-P} of 250 V), the robot takes off along the guide rails vertically as shown in Fig. 11.

A control experiment is included that such robot without wing membrane (mass of the wing membrane is small and can be neglected) cannot generate any movement along the guide rails no matter the guide rails are horizontally or vertically.

4. Discussions and conclusions: This Letter has systematically presented a novel method for creating insect-scale flapping-wing robots, which has taken into account the assembly issues among micro components. By using this method, the piezoelectric actuator processes highly evaluated performance as shown from the experimental results. The assembly between the transmission and the airframe is successfully avoided. High-performance artificial wings are obtained by reasonably arranging the fibre directions of the carbon fibre. Finally, a piezoelectric driven, sub 100 mg, insect-scale self-lifting flapping-wing robot is created,

showing that this method demonstrates high feasibility and novelty for insect-scale flapping-wing robots.

5. Acknowledgments: This work was supported by the Supporting Foundation of the Ministry of Education (62501040303), the Pre-research Fund (9140A26020313JW03371, 9140A26020414JW03412, 301020803, 010701) and the New Century Excellent Talents Support Program from the Ministry of Education of China (NCET-10-0583).

6 References

- [1] Ellington C.P.: 'The aerodynamics of hovering insect flight. IV. Aerodynamic mechanisms', *Philos. Trans. R. Soc. Lond B Biol. Sci.*, 1984, **305**, (1122), pp. 79–113
- [2] Sane S.P.: 'The aerodynamics of insect flight', *J. Exp. Biol.*, 2003, **206**, (23), pp. 4191–4208
- [3] Liu H., Ravi S., Kolomenskiy D., *ET AL.*: 'Biomechanics and biomimetics in insect-inspired flight systems', *Phil. Trans. R. Soc. B*, 2016, **371**, (1704), doi: 10.1098/rstb.2015.0390
- [4] Wood R.J.: 'The first takeoff of a biologically inspired at-scale robotic insect', *IEEE Trans. Robot.*, 2008, **24**, (2), pp. 341–347
- [5] Keennon M., Klingebiel K., Won H., *ET AL.*: 'Development of the nano hummingbird: a tailless flapping wing micro air vehicle'. AIAA Aerospace Sciences Meeting. AIAA Reston, VA, January 2012, pp. 1–24
- [6] Roll J.A., Cheng B., Deng X.: 'Design, fabrication, and experiments of an electromagnetic actuator for flapping wing micro air vehicles'. IEEE Int. Conf. on Robotics and Automation (ICRA), May 2013, pp. 809–815
- [7] Roll J.A., Cheng B., Deng X.: 'An electromagnetic actuator for high-frequency flapping-wing microair vehicles', *IEEE Trans. Robot.*, 2015, **31**, (2), pp. 400–414
- [8] Zou Y., Zhang W., Zhang Z.: 'Liftoff of an electromagnetically driven insect-inspired flapping-wing robot', *IEEE Trans. Robot.*, 2016, **32**, (5), pp. 1285–1289
- [9] Yang L.J., Jan D.L., Lin W.C.: 'Steel-based bionic actuators for flapping microair-vehicles', *Micro Nano Lett.*, 2013, **8**, (10), pp. 686–690
- [10] Rosen M.H., le Pivain G., Sahai R., *ET AL.*: 'Development of a 3.2 g untethered flapping-wing platform for flight energetics and control experiments'. IEEE Int. Conf. on Robotics and Automation (ICRA), May 2016, pp. 3227–3233
- [11] Nguyen Q.V., Chan W.L., Debiase M.: 'Hybrid design and performance tests of a hovering insect-inspired flapping-wing micro aerial vehicle', *J. Bionic. Eng.*, 2016, **13**, (2), pp. 235–248